

See discussions, stats, and author profiles for this publication at: <https://www.researchgate.net/publication/7488027>

# SAR by MS: Discovery of a New Class of RNA-Binding Small Molecules for the Hepatitis C Virus: Internal Ribosome Entry Site IIA Subdomain

ARTICLE in JOURNAL OF MEDICINAL CHEMISTRY · DECEMBER 2005

Impact Factor: 5.45 · DOI: 10.1021/jm050815o · Source: PubMed

---

CITATIONS

79

---

READS

51

12 AUTHORS, INCLUDING:



**Punit P Seth**

Ionis Pharmaceuticals

63 PUBLICATIONS 1,122 CITATIONS

SEE PROFILE



**Kristin Sannes Lowery**

Ibis Biosciences

60 PUBLICATIONS 2,011 CITATIONS

SEE PROFILE



**Christian Massire**

Ibis Biosciences

49 PUBLICATIONS 2,427 CITATIONS

SEE PROFILE

# SAR by MS: Discovery of a New Class of RNA-Binding Small Molecules for the Hepatitis C Virus: Internal Ribosome Entry Site IIA Subdomain

Punit P. Seth,\* Alycia Miyaji, Elizabeth A. Jefferson, Kristin A. Sannes-Lowery, Stephen A. Osgood, Stephanie S. Propp, Ray Ranken, Christian Massire, Rangarajan Sampath, David J. Ecker, Eric E. Swayze, and Richard H. Griffey

*Ibis Therapeutics, A Division of Isis Pharmaceuticals Inc., 1891 Rutherford Road, Carlsbad, California 92008*

Received August 16, 2005

**Abstract:** A new class of small molecules that bind the HCV RNA IRES IIA subdomain with sub-micromolar affinity is reported. The benzimidazole ‘hit’ **1** with a  $K_D \sim 100 \mu\text{M}$  to a 29-mer RNA model of Domain IIA was identified from a 180000-member library using mass spectrometry-based screening methods. Further MS-assisted SAR (structure–activity relationships) studies afforded benzimidazole derivatives with sub-micromolar binding affinity for the IIA RNA construct. The optimized benzimidazoles demonstrated activity in a cellular replicon assay at concentrations comparable to their  $K_D$  for the RNA target.

It is estimated that hepatitis C virus (HCV) has infected more than 170 million people worldwide, nearly five times more than human immunodeficiency virus (HIV).<sup>1</sup> These infections frequently become chronic and often lead to liver cirrhosis or cancer. Current therapies, either interferon (IFN)- $\alpha$  monotherapy or a combination of IFN- $\alpha$  with ribavirin, are effective at treating only a subgroup of HCV-infected patients and are frequently associated with serious side effects. As a result, new therapies for the treatment of HCV are highly desirable.<sup>2,3</sup>

HCV is a small, enveloped, positive-stranded RNA virus from the Flaviviridae family.<sup>4</sup> The HCV genome is composed of a highly conserved 340 nucleotide 5'-UTR (untranslated region), a single open reading frame (ORF) of  $\sim 9000$  nucleotides, and a short 3'-UTR. The 5'-UTR contains an internal ribosome entry site (IRES), which mediates the initiation of viral-RNA translation in a cap-independent manner.<sup>5</sup> Even though the HCV-IRES presents an exciting opportunity for developing novel HCV therapeutics,<sup>6</sup> it remains a largely unexplored drug target for small molecules.<sup>3</sup> With the exception of complex RNA-binding natural antibiotics and organic cations, discovery of new classes of small molecules that bind structured RNA targets with specificity and selectivity has been difficult.<sup>7–11</sup> The paucity of RNA-focused medicinal chemistry efforts has also contributed to a poor understanding of the general principles that govern the recognition of RNA by small molecules.<sup>7</sup> In this report, we describe the use of SAR by MS<sup>12</sup> methods, to discover a new class of small molecules with high affinity for the HCV-IRES IIA subdomain.

We started with the IIA subdomain as the focus for high throughput screening (HTS), using a 29-mer RNA construct as the target (Figure 1). The stem II of the

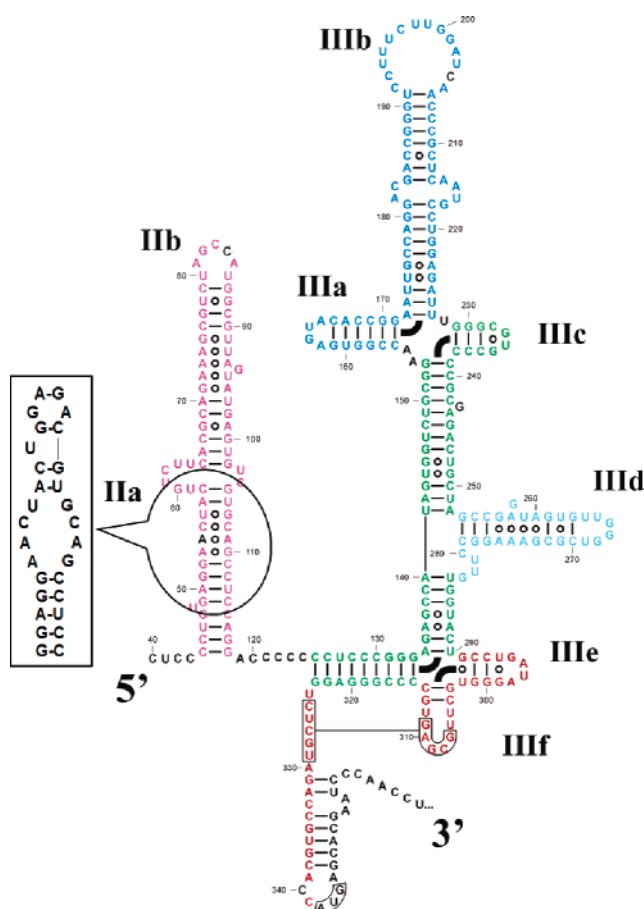


**Figure 1.** Secondary structure of HCV-IRES and 29-mer IIA screening RNA.

HCV-IRES is known to be important for IRES dependent translation, as well as for HCV RNA replication. Cryoelectron microscopy mapping of the HCV-IRES bound to the 40S ribosomal subunit shows that stem II induces a conformation change in the 40S ribosomal subunit and positions the single-stranded coding RNA into the decoding site.<sup>13</sup> Mutation studies of the different bulge regions of domain II have also demonstrated the importance of stem II for HCV replication and translation in a cell culture system.<sup>14,15</sup>

Mass spectrometry-based high throughput screening<sup>16–19</sup> of our compound collection against the IIA 29-mer (in the presence of a 33-mer structured RNA control) led to the identification of the benzimidazole ‘hit’ **1** (Table 1) displaying modest affinity and selectivity for the target RNA.<sup>20</sup> Our initial SAR plan for optimizing benzimidazole **1** involved investigating the importance of the dimethylamino headgroup on the tether at N1 as well as introducing electron-withdrawing and donating groups on the benzimidazole ring ( $\sim 150$  analogues prepared).<sup>21</sup>

The dimethylamino headgroup on the tether at N1 was found to be critical for RNA-binding as removal of this group resulted in a significant loss of binding affinity (Table 1, **2a**). Replacement of the dimethylamino group with other cationic headgroups such as pyrrolidino, diethylamino, and morpholino (**2b–d**) resulted in a slight to substantial loss of binding affinity, whereas

**Table 1.** N1 Head group SAR for Selected Analogues

compd	R	$K_D$ 29-mer ( $\mu$ M)	MS selectivity
<b>1</b>	Me <sub>2</sub> N	100	3
<b>2a</b>	H	>200	1
<b>2b</b>	1-pyrrolidino	125	3
<b>2c</b>	Et <sub>2</sub> N	130	3
<b>2d</b>	4-morpholino	>200	1
<b>2e</b>	( <i>n</i> -butyl) <sub>2</sub> N	>200	1

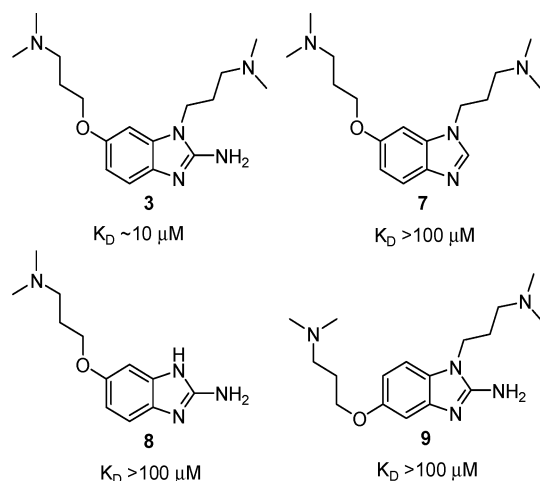
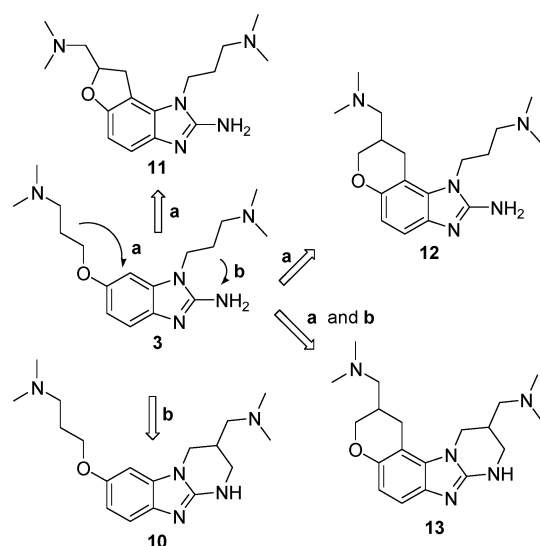
**Table 2.** Alkoxy Group SAR for Selected Analogues

compd	R	$K_D$ 29-mer ( $\mu$ M)	MS selectivity
<b>2f</b>	6-OMe	40	6
<b>2g</b>	4-OMe	>200	1
<b>2h</b>	5-OMe	>200	1
<b>2i</b>	7-OMe	50	4
<b>2j</b>	6-OBn	99	6
<b>3</b>	6-(Me <sub>2</sub> NCH <sub>2</sub> CH <sub>2</sub> CH <sub>2</sub> O)	10	15
<b>4</b>	6-(Me <sub>2</sub> NCH <sub>2</sub> CH <sub>2</sub> O)	8	11
<b>5</b>	6-[(Me <sub>2</sub> N)(CH <sub>2</sub> ) <sub>4</sub> O]	7	7
<b>6</b>	6-(Me <sub>2</sub> CHCH <sub>2</sub> CH <sub>2</sub> O)	48	6

the bulky dibutyl group led to a total loss of binding (**2e**). Reducing the length of the tether between the headgroup and the benzimidazole nucleus also resulted in a 2-fold loss of binding affinity (data not shown). From the above results it was concluded that the dimethylaminopropyl chain at N1 was optimal for RNA binding.

Introduction of a variety of substituents at the C5 and C6 positions of the benzimidazole nucleus resulted in a substantial decrease in binding affinity (data not shown). The only substituent that resulted in a slight improvement of binding affinity was a methoxy group at C6 (Table 2, **2f**). To further probe the effect of the methoxy group on RNA-binding, benzimidazoles **2g–i** with methoxy groups at C4, C5, and C7 were prepared and evaluated. While the introduction of the methoxy group at C7 was tolerated, the introduction of this substituent at C4 and C5 did not have any beneficial effect on binding. Presumably, the binding pocket in the RNA is not spacious enough to accommodate substitution at the C4 and C5 positions of the benzimidazole nucleus.

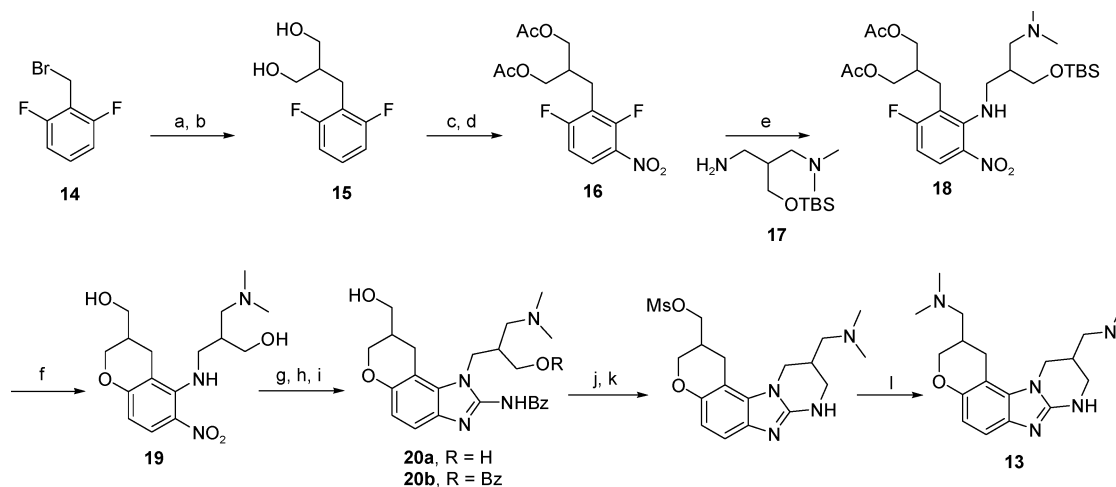
To further evaluate the effect of alkoxy substitution at the C6 position, a number of benzimidazoles substituted at this position were prepared and evaluated for binding in the MS assay. Introduction of a benzyl group (**2j**) as well as a variety of other alkyl chains on the oxygen atom at C6 did not provide any improvement in binding affinity (data not shown). Interestingly, introduction of a 3-(dimethylamino)propyloxy side chain at C6 in compound **3** provided a roughly 10-fold increase in binding affinity and a 5-fold increase in selectivity for the 29-mer IIA target. Replacement of the propyl linker between the cationic headgroup and the oxygen atom with an ethyl or butyl linker provided analogues with similar binding affinities for the RNA but reduced

**Figure 2.** Analogues used to probe specificity of binding contacts for benzimidazole **3**.**Figure 3.** Strategy for preparing conformationally restricted benzimidazoles.

selectivity (**4** and **5**). In contrast, removal of the charge by substitution of the nitrogen atom in side chain with carbon (**6**) resulted in a loss of binding affinity.

To eliminate the possibility that the increase in binding affinity was a result of nonspecific interaction of the cationic side-chains with the RNA, benzimidazoles **7**, **8**, and **9** (Figure 2) were prepared and screened in the MS assay. Gratifyingly, none of the above compounds showed any significant binding to the IIA target ( $K_D > 100 \mu\text{M}$ ), indicating that the 2-amino group and the cationic side chains at N1 and C6 were all forming specific contacts with the RNA.

In the next round of optimization, we identified a number of motifs as potential replacements for the dimethylamino headgroup at the C6 position. However, the motifs that provided the most dramatic increases in binding affinity tended to be polycationic in nature and resulted in compounds that were deemed too polar for potential therapeutic applications (data not shown). An alternate strategy to optimize binding of benzimidazole **3** to the IIA target constrained the flexible side chains<sup>22</sup> at N1 and C6 into the benzimidazole nucleus to provide compounds **10**, **11**, **12**, and **13** (Figure 3).

Scheme 1<sup>a</sup>

<sup>a</sup> Reagents and conditions: (a) NaH, Diethyl malonate, THF,  $-78^{\circ}\text{C}$  – rt; (b) LAH, THF,  $-78^{\circ}\text{C}$  – rt (70% over two steps); (c) acetyl chloride,  $\text{CH}_2\text{Cl}_2$ ,  $\text{Et}_3\text{N}$ , DMAP; (d) fuming  $\text{HNO}_3$ ,  $0^{\circ}\text{C}$ , 30 min.; (e) **17**,  $\text{CH}_2\text{Cl}_2$ ,  $\text{CaCO}_3$ , rt, 16 h; (f) dry DMSO, MeOH,  $\text{K}_2\text{CO}_3$ ,  $50^{\circ}\text{C}$ , 54 h (25% over four steps); (g) Pd/C,  $\text{H}_2$  balloon, MeOH; (h) BzNCS, DIPEA,  $\text{CH}_2\text{Cl}_2$ ; (i) EDC,  $\text{CH}_2\text{Cl}_2$  (57% over three steps); (j) 10% HCl, dioxane, reflux, 8 h; (k)  $\text{CH}_2\text{CO}_2\text{Cl}$ ,  $\text{Et}_3\text{N}$ , DMAP,  $\text{CH}_2\text{Cl}_2$ ; (l) 40%  $\text{Me}_2\text{NH}/\text{H}_2\text{O}$ , DMF,  $40^{\circ}\text{C}$ .

The synthetic route used to prepare the double-constrained benzimidazole **13** is described in Scheme 1. Reaction of benzyl bromide **14** with the sodium salt of diethyl malonate followed by reduction of the alkylated diester with LAH provided diol **15** (70% over two steps). Protection of diol **15** with acetyl chloride followed by nitration with fuming nitric acid provided compound **16**. Selective  $\text{S}_{\text{N}}\text{Ar}$  displacement of the *o*-fluorine with amine **17** provided nitroaniline **18**. A one-pot deprotection of the acetyl groups followed by intramolecular cyclization of the released diol provided benzopyran **19** (25% yield from **15**). Further elaboration of benzopyran **19** to the protected benzimidazole **20** was carried out as described previously.<sup>23</sup> Deprotection of the benzoyl protecting group in **20** was accomplished by refluxing in 10% aq HCl/dioxane. Treatment of the crude mixture above with methanesulfonyl chloride resulted in cyclization to the double-constrained benzimidazole nucleus as well as mesylation of the primary hydroxyl group on the benzopyran ring. Subsequent displacement with 40% aq dimethylamine provided the desired benzimidazole **13** after purification by reverse phase preparative HPLC.

While this work was in progress, an NMR structure of domain II was published.<sup>24</sup> This structure supported a fold of stem II<sup>25</sup> different from the previously proposed structure<sup>26,27</sup> and called into question the relevance of our original binding data. To address this, we designed a construct which contains residues 49–67 on the 5'-side and 100–114 on the 3'-side of the HCV 5'-UTR. This 40-mer RNA (Figure 4) contains the key stem IIa region, yet allows either of the folds proposed in the literature. We found that compound **3** bound to the 40-mer RNA with a  $K_D$  of 17  $\mu\text{M}$ , only slightly weaker than the 10  $\mu\text{M}$  observed for the 29-mer. Further studies are in progress to characterize the nature of the structures of the 29-mer and 40-mer stem IIa screening constructs.

All the constrained benzimidazoles showed significantly improved binding to the 40-mer RNA model of IIA (Table 3). Constraining the N1 side chain (**10**) provided a roughly 3-fold increase in binding affinity relative to benzimidazole **3**. The effect of constraining

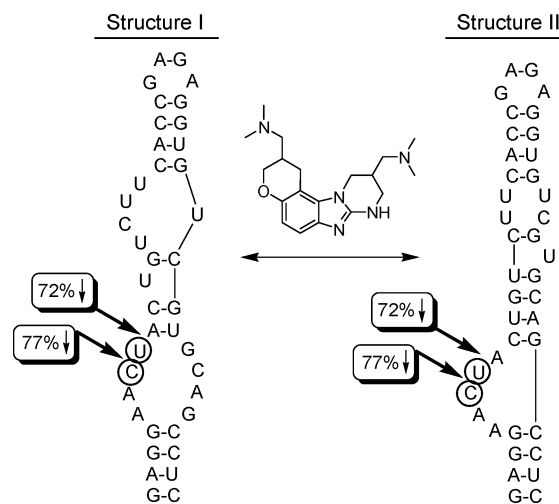


**Figure 4.** Mapping data for benzimidazole **13** to 40-mer IIA screening RNA. Protection from enzymatic digestion by RNase A in the presence of **13** is observed in the lower bulge region of the stem IIa structure. Structure I was proposed based on chemical and enzymatic probing,<sup>26,27</sup> and Structure II was proposed based on genetic analysis<sup>25</sup> and subsequently identified by NMR studies.

**Table 3.** MS Binding, Replicon Activity and Cellular Toxicity of Selected Benzimidazoles

compd	MS $K_D$ 40-mer ( $\mu\text{M}$ )	replicon $\text{EC}_{50}$ ( $\mu\text{M}$ )	MTT (Huh-7) $\text{CC}_{50}$ ( $\mu\text{M}$ )
<b>1</b>	>100	NT	>100
<b>3</b>	17	37	>100
<b>10</b>	3.5	29	>100
<b>11</b>	1.7	1.5	>100
<b>12</b>	0.86	3.9	>100
<b>13</b>	0.72	5.4	>100

the C6 side chain as a benzofuran (**11**) or benzopyran (**12**) ring was more spectacular and produced a 10-fold or a 20-fold increase respectively, in binding affinity relative to benzimidazole **3**. The doubly constrained benzimidazole **13** (racemic mixture of cis and trans diastereomers) proved to have the highest affinity in this series with a measured  $K_D$  of 0.72  $\mu\text{M}$ . This was a 25-fold increase in binding affinity relative to benzim-



idazole **3** and 140-fold overall increase in binding affinity relative to the initial hit **1**.<sup>28</sup>

The binding site of benzimidazole **13** on the 40-mer RNA was further investigated by a RNA footprinting experiment using RNase A digestion (Figure 4). The 40-mer RNA was incubated with RNase A without any ligand and the cleavage sites were identified. In the presence of benzimidazole **13**, the backbone phosphates in the internal loop were strongly protected (>70% reduction in RNA cleavage) from enzymatic cleavage at the sites shown in Figure 4. This experiment provides additional evidence that the benzimidazoles are binding specifically in a pocket created by the three-dimensional architecture of the RNA.

The optimized benzimidazoles were finally tested for activity in an HCV-replicon assay<sup>29</sup> where they reduced HCV RNA levels, as measured by RT-PCR, at low micromolar concentrations. Notably, the SAR trends seen in the replicon assay were similar to those observed in the MS assay. The slightly better activity in the cellular replicon assay seen with benzimidazole **11** could be attributed to enhanced cellular penetration properties of this analogue. All the benzimidazole compounds also showed minimal toxicity (CC<sub>50</sub> > 100  $\mu$ M) against Huh-7 cells in an MTT assay.

In conclusion, using mass spectrometry screening as a tool to guide SAR, we have developed a new class of small molecules with high affinity for the HCV-IRES IIA subdomain. The optimized benzimidazoles reduced viral RNA in a cellular replicon assay at concentrations comparable to the binding constants observed in the MS assay. Further investigation into the mechanism by which the benzimidazoles elicit their biological activity is in progress and will be reported in due course.

**Acknowledgment.** We thank Dr. Stanley Crooke for many helpful discussions and Dr. Erich Koller and Dr. Larry Blynn for assistance with the replicon assay.

**Supporting Information Available:** Detailed experimental procedures for the preparation of compounds **11**, **12**, and **13**, along with a description of procedures used for the cellular assays, the MS binding assay, and MS mapping experiment for benzimidazole **13**. This material is available free of charge via the Internet at <http://pubs.acs.org>.

## References

- Lauer, G. M.; Walker, B. D. Hepatitis C Virus Infection. *N. Engl. J. Med.* **2001**, *345*, 41–52.
- Strader, D. B.; Wright, T.; Thomas, D. L.; Seeff, L. B. Diagnosis, Management, and Treatment of Hepatitis C. *Hepatology* **2004**, *39*, 1147–1171.
- Tan, S.-L.; Pause, A.; Shi, Y.; Sonenberg, N. Hepatitis C therapeutics: current status and emerging strategies. *Nat. Rev. Drug Discovery* **2002**, *1*, 867–881.
- Major, M. E.; Feinstone, S. M. The Molecular Virology of Hepatitis C. *Hepatology* **1997**, *25*, 1527–1538.
- Kieft, J. S.; Zhou, K.; Jubin, R.; Doudna, J. A. Mechanism of ribosome recruitment by hepatitis C IRES RNA. *RNA* **2001**, *7*, 194–206.
- Gallego, J.; Varani, G. The hepatitis C virus internal ribosome entry site: a new target for antiviral research. *Biochem. Soc. Trans.* **2002**, *30*, 140–146.
- Gallego, J.; Varani, G. Targeting RNA with Small-Molecule Drugs: Therapeutic Promise and Chemical Challenges. *Acc. Chem. Res.* **2001**, *34*, 836–843.
- Sucheck, S. J.; Wong, C.-H. RNA as a target for small molecules. *Curr. Opin. Chem. Biol.* **2000**, *4*, 678–686.
- Wilson, W. D.; Li, K. Targeting RNA with small molecules. *Curr. Med. Chem.* **2000**, *7*, 73–98.
- Chow, C. S.; Bogdan, F. M. A Structural Basis for RNA-Ligand Interactions. *Chem. Rev.* **1997**, *97*, 1489–1513.
- Tor, Y. Targeting RNA with small molecules. *ChemBioChem* **2003**, *4*, 998–1007.
- Swayze, E. E.; Jefferson, E. A.; Sannes-Lowery, K. A.; Blyn, L. B.; Risen, L. M.; Arakawa, S.; Osgood, S. A.; Hofstadler, S. A.; Griffey, R. H. SAR by MS: A Ligand Based Technique for Drug Lead Discovery Against Structured RNA Targets. *J. Med. Chem.* **2002**, *45*, 3816–3819.
- Spahn, C. M.; Kieft, J. S.; Grassucci, R. A.; Penczek, P. A.; Zhou, K.; Doudna, J. A.; Frank, J. Hepatitis C virus IRES RNA-induced changes in the conformation of the 40s ribosomal subunit. *Science* **2001**, *291*, 1959–1962.
- Odreman-Macchioli, F.; Baralle, F. E.; Buratti, E. Mutational Analysis of the Different Bulge Regions of Hepatitis C Virus Domain II and Their Influence on Internal Ribosome Entry Site Translational Ability. *J. Biol. Chem.* **2001**, *276*, 41648–41655.
- Kalliampakou, K. I.; Psaridi-Linardaki, L.; Mavromara, P. Mutational analysis of the apical region of domain II of the HCV IRES. *FEBS Lett.* **2002**, *511*, 79–84.
- Hofstadler, S. A.; Sannes-Lowery, K. A.; Crooke, S. T.; Ecker, D. J.; Sasmor, H.; Manalili, S.; Griffey, R. H. Multiplexed Screening of Neutral Mass-Tagged RNA Targets against Ligand Libraries with Electrospray Ionization FTICR MS: A Paradigm for High-Throughput Affinity Screening. *Anal. Chem.* **1999**, *71*, 3436–3440.
- Sannes-Lowery, K. A.; Drader, J. J.; Griffey, R. H.; Hofstadler, S. A. High-performance mass spectrometry as a drug discovery tool: a high-throughput screening assay to identify RNA-binding ligands. *Proc. SPIE-Int. Soc. Opt. Eng.* **2001**, *4264*, 27–36.
- Sannes-Lowery, K. A.; Drader, J. J.; Griffey, R. H.; Hofstadler, S. A. Fourier transform ion cyclotron resonance mass spectrometry as a high throughput affinity screen to identify RNA binding ligands. *TrAC, Trends Anal. Chem.* **2000**, *19*, 481–491.
- Sannes-Lowery, K. A.; Griffey, R. H.; Hofstadler, S. A. Measuring Dissociation Constants of RNA and Aminoglycoside Antibiotics by Electrospray Ionization Mass Spectrometry. *Anal. Biochem.* **2000**, *280*, 264–271.
- In our assay a hit is described as a ligand with a dissociation constant of 100  $\mu$ M or less and a selectivity of 3 or greater for the target RNA. Selectivity is defined as the ratio of ligand dissociation constant for the 33-mer vs the 29-mer RNA.
- Seth, P. P.; Jefferson, E. A.; Griffey, R. H.; Swayze, E. E. Benzimidazoles and analogs thereof as antivirals. PCT Int. Appl. WO 2004050035, 2004.
- Hart, P. A.; Rich, D. H. Stereochemical aspects of drug action I: conformational restriction, steric hindrance, and hydrophobic collapse. In *Practice of Medicinal Chemistry*; Wermuth, C. G., Ed.; Academic Press: San Diego, 1996; pp 393–412.
- Seth, P. P.; Robinson, D. E.; Jefferson, E. A.; Swayze, E. E. Efficient solution phase synthesis of 2-(N-acyl)-aminobenzimidazoles. *Tetrahedron Lett.* **2002**, *43*, 7303–7306.
- Lukavsky, P. J.; Kim, I.; Otto, G. A.; Puglisi, J. D. Structure of HCV IRES domain II determined by NMR. *Nat. Struct. Biol.* **2003**, *10*, 1033–1038.
- Zhao, W. D.; Wimmer, E. Genetic analysis of a poliovirus/hepatitis C virus chimera: new structure for domain II of the internal ribosomal entry site of hepatitis C virus. *J. Virol.* **2001**, *75*, 3719–3730.
- Kieft, J. S.; Zhou, K.; Jubin, R.; Murray, M. G.; Lau, J. Y.; Doudna, J. A. The Hepatitis C Virus Internal Ribosome Entry Site Adopts an Ion-dependent Tertiary Fold. *J. Mol. Biol.* **1999**, *292*, 513–529.
- Honda, M.; Beard, M. R.; Ping, L. H.; Lemon, S. M. A phylogenetically conserved stem-loop structure at the 5' border of the internal ribosome entry site of hepatitis C virus is required for cap-independent viral translation. *J. Virol.* **1999**, *73*, 1165–1174.
- The optimized benzimidazoles typically displayed 30–50-fold selectivity for the IIA target over other RNA subdomains used in the screening assay.
- Yi, M.; Bodola, F.; Lemon, S. M. Subgenomic hepatitis C virus replicons inducing expression of a secreted enzymatic reporter protein. *Virology* **2002**, *304*, 197–210.

JM0508150